Chapter 6

Models of compact stars on paraboloidal spacetime satisfying Karmarkar condition

Exact solutions of Einstein's field equations on the background of paraboloidal spacetime using Karmarkar condition is obtained. The physical acceptability conditions of the model are investigated and found that the model is compatible with a number of compact star candidates like Her X-1, LMC X-4, EXO 1785-248, PSR J1903+327, Vela X-1 and PSR J1614-2230. A noteworthy feature of the model is that it is geometrically significant and simple in form.

6.1 Introduction

Ever since Schwarzschild obtained exact solution of EFEs, a wide variety of exact solutions with physical significance and devoid of any physical significance were given by a number of researchers. The analysis of solutions for physical significance revealed that out of 127 exact solutions, only 16 could withstand the elemen-

tary test for physical acceptability of the solutions (Delgaty and Lake [1998]). By the discovery of superdense stars like neutron stars and pulsars a new interest has emerged among researchers for developing mathematical models of such distributions. It has been suggested, theoretically, by Ruderman [1972] and Canuto [1974] that, stars, whose density in the range greater than $10^{15}gm/cm^3$ may develop pressure anisotropy within it.

Bowers and Liang [1974] has discussed diverse reasons for the occurrence of anisotropy inside the star. They have shown that anisotropy can affect the maximum equilibrium mass and surface redshift of the distribution. Since then, a number of anisotropic models of superdense stars have been developed and investigated (Maharaj and Maartens [1989], Gokhroo and Mehra [1994], Patel and Mehta [1995], Tikekar and Thomas [1998, 1999, 2005], Thomas et al. [2005], Thomas and Ratanpal [2007]). Impacts of anisotropy on the stability of a stellar configuration have been studied by Dev and Gleiser [2002, 2003, 2004]. Sharma and Maharaj [2007] and Thirukkanesh and Maharaj [2008] have obtained analytic solutions of compact anisotropic stars by assuming a linear equation of state(EOS). To solve the Einstein-Maxwell system, Komathiraj and Maharaj [2007a] have used a linear equation of state. By assuming a linear EOS, Sunzu et al. [2014] have reported solutions for a charged anisotropic quark star. Feroze and Siddiqui [2011] and Maharaj and Takisa [2012] have used a quadratic-type EOS for obtaining solutions of anisotropic distributions. Varela et al. [2010] have analyzed charged anisotropic configurations admitting a linear as well as non-linear equations of state. For a star composed of quark matter in the MIT bag model, Paul et al. [2011] have shown how anisotropy could effect the value of the Bag constant. For a specific polytropic index, exact solutions to Einstein's field equations for an anisotropic sphere admitting a polytropic EOS have been obtained by Thirukkanesh and Ragel [2012]. Maharaj and Takisa [2013] have used the same type of EOS to develop an analytical model describing a

charged anisotropic sphere.

Bhar [2015a,b] and Singh and Pant [2015] have shown that pressure anisotropy leads to arbitrarily large red-shifts. There has been a renewed interest among researchers to develop spacetime metrics of stellar objects of embedding class one type spacetimes (Karmarkar [1948]). Solutions representing superdense stars of embedding class one which are compatible with observational data of pulsars have been given by Bhar et al. [2016], Singh and Pant [2016], Singh et al. [2017a,b,c].

6.2   Solution of Field Equations Using Karmarkar Condition

We shall consider the spacetime metric

$$ds^2 = e^{\nu(r)}dt^2 - e^{\lambda}dr^2 - r^2d\theta^2 - r^2sin^2\theta \ d\phi^2 \tag{6.1}$$

with

$$e^{\lambda} = \left(1 + \frac{r^2}{R^2}\right) \tag{6.2}$$

for describing the interior of anisotropic fluid distribution. A detailed study of the metric (6.1) with (6.2) has been done by Jotania and Tikekar [2006].

The energy-momentum tensor for anisotropic matter distribution is taken as

$$T_i^j = (\rho + p_r)u^j u_i - p_\perp \delta_i^j + (p_r - p_\perp)\eta^j \eta_i \tag{6.3}$$

where u_i denotes the four-velocity and η_i is a space like vector orthogonal to u^i satisfying the conditions

$$u^j u_i = 1, \ \eta^j \eta_i = -1 \text{ and } u^j \eta_i = 0. \tag{6.4}$$

$\rho, p_r, p_\perp$ denotes the proper density, the radial pressure and the transverse pressure, respectively.

The Einstein's field equations for the metric (6.1) along with the ansatz (6.2) with energy-momentum tensor (6.3) are equivalent to the following set of three equations

$$8\pi\rho = \frac{e^{-\lambda}\lambda'}{r} + \frac{1-e^{-\lambda}}{r^2}, \tag{6.5}$$

$$8\pi p_r = \frac{e^{-\lambda}\nu'}{r} + \frac{e^{-\lambda}-1}{r^2}, \tag{6.6}$$

$$8\pi p_\perp = e^{-\lambda}\left(\frac{\nu''}{2} + \frac{\nu'^2}{4} - \frac{\nu'\lambda'}{4} + \frac{\nu'-\lambda'}{2r}\right). \tag{6.7}$$

Equations (6.5) – (6.7) consist of a system of three equations in five unknowns $(\lambda, \nu, \rho, p_r, p_\perp)$. One of the variables λ is known from (6.2). Once we know the value of ν, the values of $\rho, p_r, p_\perp$ can be obtained from equations (6.5), (6.6) and (6.7). The spacetime metric (6.1) is of class one type if it satisfies the Karmarkar condition [Karmarkar, 1948] given by

$$R_{1414}R_{2323} = R_{1212}R_{3434} + R_{1224}R_{1334} \tag{6.8}$$

with $R_{2323} \neq 0$ where components of Riemann curvature tensor are given by

$$R_{2323} = r^2 sin^2\theta \left[1 - e^{-\lambda}\right],$$

$$R_{1212} = \frac{1}{2}\lambda'r,$$

$$R_{1334} = R_{1224} \; sin^2\theta = 0,$$

$$R_{1414} = -e^\nu \left[\frac{\nu''}{2} + \frac{\nu'^2}{4} - \frac{1}{4}\lambda'\nu'\right],$$

$$R_{2424} = -\frac{1}{4}\nu're^{\nu-\lambda},$$

$$R_{3434} = sin^2\theta R_{2424}.$$

The Karmarkar condition (6.8) leads to the differential equation

$$\frac{2\nu''}{\nu'} + \nu' = \frac{\lambda' e^{\lambda}}{e^{\lambda} - 1} \tag{6.9}$$

Using the expression of e^{λ} given in (6.2), equation (6.9) becomes

$$\frac{2\nu''}{\nu'} + \nu' = \frac{2}{r} \tag{6.10}$$

which gives a closed form solution

$$e^{\nu} = \left(A + B\frac{r^2}{R^2} \right)^2. \tag{6.11}$$

The explicit form of the spacetime metric is

$$ds^2 = \left(A + B\frac{r^2}{R^2} \right)^2 dt^2 - \left(1 + \frac{r^2}{R^2} \right) dr^2 - r^2 d\theta^2$$
$$-r^2 sin^2\theta \ d\phi^2, \tag{6.12}$$

where A and B are constants of integration which are to be determined using appropriate boundary conditions.

6.3 Solution of Field Equations

The field equations (6.5) – (6.7) can now be solved by using the values of λ and ν given by equations (6.2) and (6.11). The expressions for ρ, p_r and $p_\perp$ and the

anisotropy factor $\Delta(= p_r - p_\perp)$ are given, respectively, by

$$8\pi\rho = \frac{3 + \frac{r^2}{R^2}}{R^2\left(1 + \frac{r^2}{R^2}\right)^2},$$

(6.13)

$$8\pi p_r = \frac{B\left(4 - \frac{r^2}{R^2}\right) - A}{R^2\left(A + B\frac{r^2}{R^2}\right)\left(1 + \frac{r^2}{R^2}\right)},$$

(6.14)

$$8\pi p_\perp = \frac{B\left(4 + \frac{r^2}{R^2}\right) - A}{R^2\left(A + B\frac{r^2}{R^2}\right)\left(1 + \frac{r^2}{R^2}\right)^2},$$

(6.15)

and

$$8\pi\Delta = \frac{\frac{r^2}{R^2}\left[B\left(2 - \frac{r^2}{R^2}\right) - A\right]}{R^2\left(A + B\frac{r^2}{R^2}\right)\left(1 + \frac{r^2}{R^2}\right)^2}.$$

(6.16)

The anisotropy Δ vanishes at $r = 0$, which is a required condition.

6.4   Boundary Conditions

The interior spacetime metric (6.1) (with 6.2) should match continuously with the Schwarzschild exterior metric given by (2.22) across the boundary $r = a$. This gives

$$1 - \frac{2M}{a} = \frac{1}{1 + \frac{a^2}{R^2}}$$

(6.17)

determining the values of the geometric parameter R in terms of a and M by the relation

$$R = a\sqrt{\frac{a}{2M} - 1}.$$

(6.18)

The total mass enclosed within the radius a is given by

$$M = \frac{\frac{a^3}{R^2}}{2\left(1 + \frac{a^2}{R^2}\right)}.$$

(6.19)

Equating the coefficients of dt^2, we get

$$1 - \frac{2M}{a} = \left(A + B\frac{r^2}{R^2} \right)^2 = \frac{1}{1 + \frac{a^2}{R^2}} \tag{6.20}$$

which gives

$$A + B\frac{a^2}{R^2} = \frac{1}{\sqrt{1 + \frac{a^2}{R^2}}}. \tag{6.21}$$

The second boundary condition is given by $p_r(r = a) = 0$. This leads to

$$-A + B\left(4 - \frac{a^2}{R^2} \right) = 0. \tag{6.22}$$

Equations (6.21) and (6.22) determine the values of A and B in the form

$$A = \frac{4 - \frac{a^2}{R^2}}{4\sqrt{1 + \frac{a^2}{R^2}}}, \tag{6.23}$$

$$B = \frac{1}{4\sqrt{1 + \frac{a^2}{R^2}}}. \tag{6.24}$$

Using (6.23) and (6.24) we rewrite equations (6.14) – (6.16) as

$$8\pi p_r = \frac{\frac{a^2}{R^2} - \frac{r^2}{R^2}}{R^2 \left(4 + \frac{r^2}{R^2} - \frac{a^2}{R^2} \right) \left(1 + \frac{r^2}{R^2} \right)}, \tag{6.25}$$

$$8\pi p_\perp = \frac{\frac{a^2}{R^2} + \frac{r^2}{R^2}}{R^2 \left(4 + \frac{r^2}{R^2} - \frac{a^2}{R^2} \right) \left(1 + \frac{r^2}{R^2} \right)^2}, \tag{6.26}$$

$$8\pi\Delta = \frac{\frac{r^2}{R^2} \left(\frac{a^2}{R^2} - \frac{r^2}{R^2} - 2 \right)}{R^2 \left(4 + \frac{r^2}{R^2} - \frac{a^2}{R^2} \right) \left(1 + \frac{r^2}{R^2} \right)^2}. \tag{6.27}$$

6.5   Physical Acceptability Conditions

A physically acceptable anisotropic stellar model must satisfy the following conditions (Kuchowicz [1972], Buchdahl [1979], Murad and Fatema [2015b], Knutsen

[1988a]):

(a). Regularity conditions

    (i). The metric potentials $e^\lambda > 0$, $e^\nu > 0$, for $0 \le r \le a$.

    (ii). $\rho(r) \ge 0$, $p_r(r) \ge 0, p_\perp(r) \ge 0$ for $0 \le r \le a$.

    (iii). $p_r(r = a) = 0$.

(b). Causality conditions

    (i). $0 \le \frac{dp_r}{d\rho} \le 1$, for $0 \le r \le a$.

    (ii). $0 \le \frac{dp_\perp}{d\rho} \le 1$, for $0 \le r \le a$.

(c). Energy conditions

    (i). $\rho - p_r - 2p_\perp \ge 0$ (strong energy condition),

    (ii). $\rho \ge p_r$, $\rho \ge p_\perp$ (weak energy conditions).

(d). Monotone decrease of physical parameters

    (i). $\frac{d\rho}{dr} \le 0$, $\frac{dp_r}{d\rho} \le 0$ for $o \le r \le a$,

    (ii). $\frac{d}{dr}\left(\frac{dp_r}{d\rho}\right) \le 0$, for $0 \le r \le a$,

    (iii). $\frac{d}{dr}\left(\frac{p_r}{\rho}\right) \le 0$ for $0 \le r \le a$.

(e). Pressure anisotropy

$\Delta(r = 0) = 0$.

(f). Mass-radius relation

According to Buchdahl [1979], the allowable mass radius relation must satisfy

the inequality $\frac{M}{R} \le \frac{4}{9}$.

(g). Redshift

The redshift $z = e^{-\frac{\nu}{2}} - 1$ must be a decreasing function of r and finite for $0 \leq r \leq a$.

(h). Stability condition

The relativistic adiabatic index $\Gamma = \frac{\rho + p_r}{p_r} \frac{dp_r}{d\rho} \geq \frac{4}{3}$ for $0 \leq r \leq R$.

6.6   Variation of Physical Parameters

The variation of density ρ with respect to the radial variable r is given by

$$8\pi \frac{d\rho}{dr} = -\frac{2}{R^2} \cdot \frac{r}{R^2} \frac{\left(5 + \frac{r^2}{R^2}\right)}{\left(1 + \frac{r^2}{R^2}\right)^3} \tag{6.28}$$

Since $\frac{d\rho}{dr} < 0$, for $0 < r \leq a$, the density distribution decreases radially outward. The gradient of radial pressure, transverse pressure and the anisotropy variable have the following expressions

$$8\pi \frac{dp_r}{dr} = -\frac{2r}{R^4} \frac{4\left(1 + \frac{r^2}{R^2}\right) + \left(\frac{a^2}{R^2} - \frac{r^2}{R^2}\right)\left(4 + \frac{r^2}{R^2} - \frac{a^2}{R^2}\right)}{\left(4 + \frac{r^2}{R^2} - \frac{a^2}{R^2}\right)^2 \left(1 + \frac{r^2}{R^2}\right)^2}, \tag{6.29}$$

$$8\pi \frac{dp_\perp}{dr} = \frac{2r}{R^4} \frac{\left[4\left(1 - \frac{r^2}{R^2}\right) - 2\frac{a^2}{R^2}\left(5 + \frac{r^2}{R^2}\right) + 2\left(\frac{a^4}{R^4} - \frac{r^4}{R^4}\right)\right]}{\left(4 + \frac{r^2}{R^2} - \frac{a^2}{R^2}\right)^2 \left(1 + \frac{r^2}{R^2}\right)^3}, \tag{6.30}$$

$$8\pi \frac{d\Delta}{dr} = \frac{2r}{R^4} \times \frac{1}{\left(4 + \frac{r^2}{R^2} - \frac{a^2}{R^2}\right)^2 \left(1 + \frac{r^2}{R^2}\right)^3} \times$$
$$\left\{\left(4 + \frac{r^2}{R^2} - \frac{a^2}{R^2}\right)\left(\frac{a^2}{R^2} - \frac{2r^2}{R^2} - \frac{r^4}{R^4} - 2\right)\right.$$
$$\left. - \frac{r^2}{R^2}\left(1 + \frac{r^2}{R^2}\right)\left(\frac{a^2}{R^2} - \frac{r^2}{R^2} - 2\right)\right\}, \tag{6.31}$$

It can be seen from equation (6.29) that $8\pi\frac{dp_r}{dr} < 0$ for $\frac{a^2}{R^2} < 4$. This indicates that radial pressure is a decreasing function of r. However due to the complexity of expressions in the right hand side of equations (6.30) and (6.31), it is difficult to obtain the sign of the terms in their right hand side. However it can be seen from equations (6.26) and (6.27) that $p_\perp$ and Δ are also decreasing functions of r. The expressions for radial and transverse speed of sound, v_r^2 and $v_\perp^2$, and $\frac{d\Delta}{d\rho}$ are given by

$$v_r^2 = \frac{dp_r}{d\rho} = \frac{\left(1+\frac{r^2}{R^2}\right)}{\left(4+\frac{r^2}{R^2}-\frac{a^2}{R^2}\right)^2\left(5+\frac{r^2}{R^2}\right)}\left[4\left(1+\frac{r^2}{R^2}\right)+\left(\frac{a^2}{R^2}-\frac{r^2}{R^2}\right)\left(4+\frac{r^2}{R^2}-\frac{a^2}{R^2}\right)\right], \quad (6.32)$$

$$v_\perp^2 = -\frac{4\left(1-\frac{r^2}{R^2}\right)-2\frac{a^2}{R^2}\left(5+\frac{r^2}{R^2}\right)+2\left(\frac{a^4}{R^4}-\frac{r^4}{R^4}\right)}{\left(4+\frac{r^2}{R^2}-\frac{a^2}{R^2}\right)^2\left(5+\frac{r^2}{R^2}\right)}, \quad (6.33)$$

$$\frac{d\Delta}{d\rho} = -\frac{1}{\left(4+\frac{r^2}{R^2}-\frac{a^2}{R^2}\right)^2\left(5+\frac{r^2}{R^2}\right)}\left[\left(4+\frac{r^2}{R^2}-\frac{a^2}{R^2}\right)\left(\frac{a^2}{R^2}-2\frac{r^2}{R^2}-\frac{r^4}{R^4}-2\right)-\frac{r^2}{R^2}\times\right.$$
$$\left.\left(1+\frac{r^2}{R^2}\right)\left(\frac{a^2}{R^2}-\frac{r^2}{R^2}-2\right)\right]. \quad (6.34)$$

6.7 Physical analysis

In order to examine the compatibility of the model with observational data, we have considered compact stars Her X-1, LMC X-4, EXO 1785-248, PSR J1903+327, Vela X-1 and PSR J1614-2230 whose mass and size are known [Gangopadhyay et al., 2013]. By taking the mass M and radius a, the value of the geometric parameter R is found from the equation (6.18). In Fig. 6.1 we have shown the variations of density against the radius. It can be seen that the density accommodated by a star increases as the compactness increases. Her X-1 accommodates minimum density whose compactness is minimum while PSR J1614-2230 has maximum density for which compactness is maximum among all compact star candidates studied. The variation of radial pressure p_r and transverse pressure $p_\perp$ are shown in Figs. 6.2

Table 6.1: The compactness $u = \frac{M}{a}$ of different stars are shown in the following table.

Star	M ($M_\odot$)	a (km)	R (km)	$u = \frac{M}{a}$
Her X-1	0.85	8.1	12.096	0.1548
LMC X-4	1.04	8.301	10.8412	0.1848
EXO 1785-248	1.3	10	10.1182	0.1917
PSR J1903+327	1.667	9.438	9.048	0.2605
Vela X-1	1.77	9.56	8.71	0.2731
PSR J1614-2230	1.97	9.69	7.91	0.2999

and 6.3 respectively. It can be seen that both p_r and $p_\perp$ decreases radially outward and they increase with compactness. In Fig. 6.4, we have shown the variation of anisotropy against radial directions. Its value is zero at the centre and $|\Delta|$ increases radially outward. The anisotropy is negative throughout the distribution. Further, the numerical value of anisotropy is more for stars with more compactness. The velocity of sound in the radial direction v_r^2 and transverse direction $v_\perp^2$ are shown in Figs. 6.5 and 6.6 respectively. From both figures it can be noticed that $0 < \frac{dp_r}{d\rho} < 1$, and $0 < \frac{dp_\perp}{d\rho} < 1$. Further these velocities are more in magnitude in more compact stars. Fig. 6.7 shows that the strong energy condition satisfies for all stars throughout the distribution. The variation of adiabatic index is displayed in Fig. 6.8. Its value is greater than $\frac{4}{3}$ throughout and the star with less compactness accommodate more Γ value. It can be noticed that as compactness increases, the value of Γ decreases. This indicates that the star become less stable due to the increase in compactness. In Fig. 6.9 we have shown the variation of redshift z in the radial direction. Stars with more compactness shows more redshift. That is while Her X-1 shows minimum redshift while PSR J1614-2230 shows max redshift among all the compact star candidates.

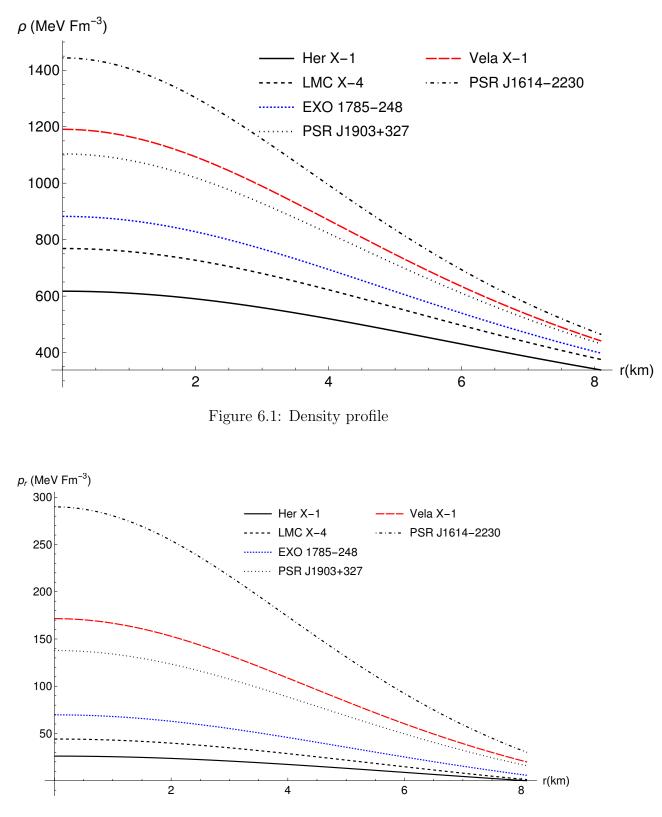Figure 6.1: Density profile

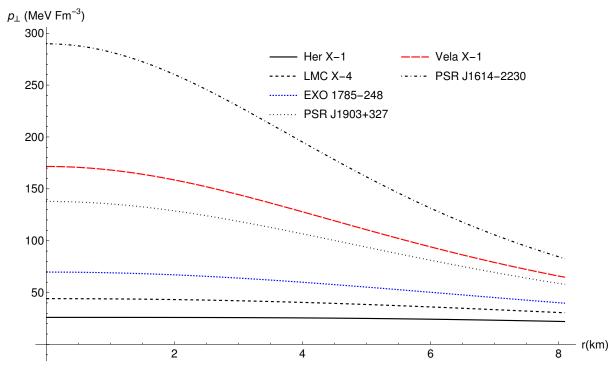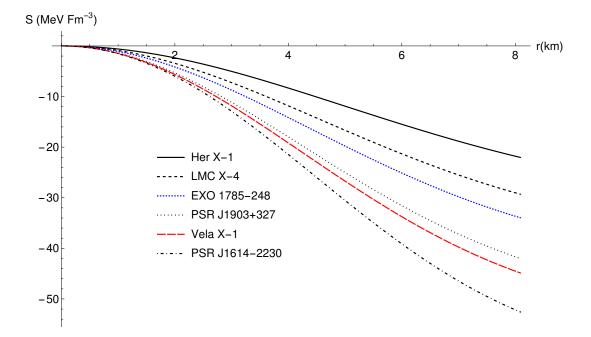Figure 6.2: Radial pressure profile

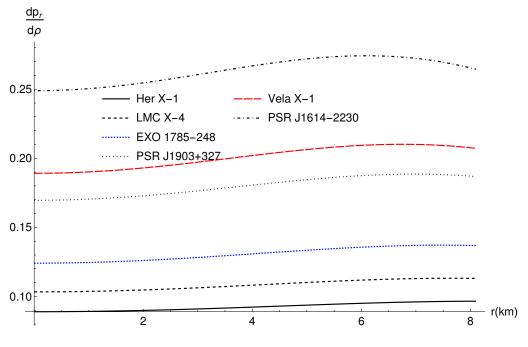Figure 6.3: Transverse pressure profile

Figure 6.4: Anisotropy profile
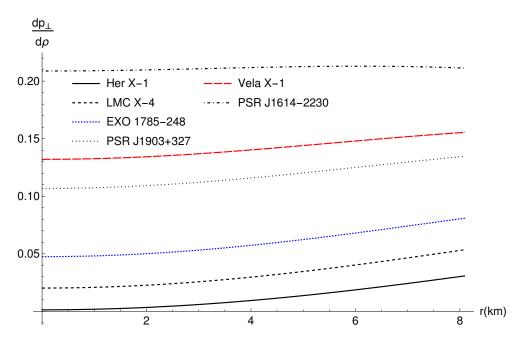
Figure 6.5: Radial sound speed profile
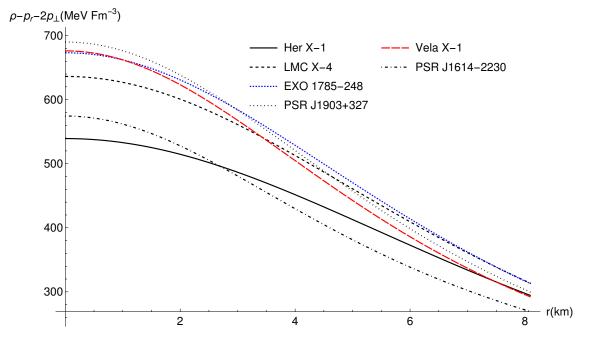

Figure 6.6: Transverse sound speed profile

$\rho - p_r - 2p_\perp (\text{MeV Fm}^{-3})$
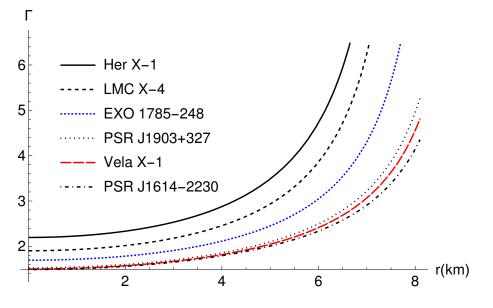
Figure 6.7: Strong energy condition profile
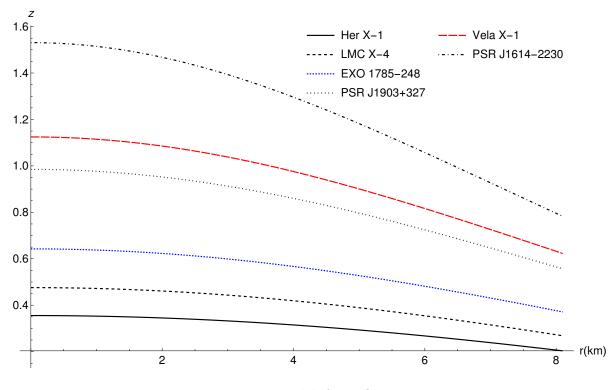
Figure 6.8: Adiabatic index profile.

Figure 6.9: Redshift profile.

6.8   Discussion

We have studied the compatibility of the model developed using Karmakar condition in the background of paraboloidal spacetime for compact stars like Her X-1, LMC X-4, EXO 1785-248, PSR J1903+327, Vela X-1 and PSR J1614-2230. It is found that our model satisfy the elementary physical requirements for representing a superdense compact star through graphical method. It is found that the model developed can accommodate the mass and radius of many of the compact star candidates given by Gangopadhyay et al. [2013].

It is found that stars whose compactness is more accommodate more density, pressure and Δ. The redshift increase with compactness while the value of Γ decreases with compactness showing that the stability decreases with increase in compactness. A pertinent feature of the model is that the exact solution obtained is simple in nature which is seldom found in many solutions. Though we have displayed here the

physical analysis, only for few compact star models, it can be applied to a larger class of known pulsars. The model possesses a definite background spacetime geometry, namely paraboloidal geometry, and the expression involved in the solution are simple in nature.